



## Experimental Investigation of the Use of Equivalent Sources Model in Room Acoustics Simulations

Yangfan LIU<sup>1</sup>; J. Stuart BOLTON<sup>2</sup>

<sup>1</sup> Ray W. Herrick Laboratories, Purdue University, USA

<sup>2</sup> Ray W. Herrick Laboratories, Purdue University, USA

### ABSTRACT

As an alternative to models based on geometrical acoustics and the computationally intensive Finite Element or Boundary Element methods, the Equivalent Sources Model (ESM) has recently been modified and extended from its original application in acoustical holography to room acoustics simulations. Previous numerical simulation results have demonstrated the advantages of room acoustics ESM's (especially when higher order sources are used as its equivalent sources) as a flexible reduced order modeling procedure in room acoustics. In the present work, an experimental investigation of the room acoustics ESM was conducted in which the sound field generated by a loudspeaker in a small room was measured. The ESM prediction of total sound field in the room is calculated by coupling a free-space ESM (which gives the source information) with a room acoustics ESM (to account for the room effect). The ESM predictions are compared with the measurements to show the validity of the room acoustics ESM in a realistic application.

Keywords: Equivalent sources, Room acoustics      I-INCE Classification of Subjects Number(s): 76.9

### 1. INTRODUCTION

The usual goal of a room acoustics simulation is to calculate the total sound field in a room with the given source information (such as the free-space sound field generated by the source and the impedance on the surface of the source) and the room condition (i.e., the impedance distribution on the room surface). In this area, there are, in general, two categories of modeling techniques: (a) wave-based models and (b) models based on geometrical acoustics. The main difference between these two model types is that the wave-based models calculate the sound field by finding a solution to the Helmholtz equation with the given impedance boundary conditions, while the methods based on geometrical acoustics predict the total sound field in a room, under the assumption of a ray representation of sound, by combining the modeling of each related acoustical phenomenon (including sound generation, propagation, reflection, diffraction, etc.). Although the wave based methods, are mathematically more rigorous, they are usually limited to the low frequency range, since the boundary value problem is typically solved by Boundary Element (1-3) or Finite Element methods (4-6), both of which require an impractically dense geometry mesh at high frequencies. Because of this limitation, the methods based on geometrical acoustics are used in most room acoustics simulation practices. However, most treatments in geometrical acoustics are, strictly speaking, high frequency approximations of waves. These approximations include modeling the source as a point source with certain directivity, sound propagation as rays, describing the sound reflection by using plane wave reflection coefficients (7), etc. Recent developments of geometrical room acoustics models, which are implemented in various commercial room acoustics software packages (8-10), often involve hybrid models combining Image Source Models (11-13) for early reflections and stochastic ray tracing (14-15) or beam tracing (16-18) models for late reflections in which scattering (19) and angle-dependent reflections (20) are also considered. In order to reduce the effort of finding the audible image source locations, a deterministic ray tracing (21) or beam tracing (10) can be used (note that this approach is sometimes referred to by other names).

---

<sup>1</sup> liu278@purdue.edu

<sup>2</sup> bolton@purdue.edu

In very recent years, the use of Equivalent Source Models has been proposed for room acoustics simulations. This wave-based method (22) is efficient in numerical calculations, can deal with non-point sources and possesses the flexibility to make a straightforward trade-off between prediction accuracy and computational burden. In this type of approach, the room component of the total sound field is assumed to be generated by certain types of equivalent sources with undetermined source strengths, and the source strengths are then estimated by matching the given impedance boundary conditions on the surfaces in the room. After the source strengths are estimated, they can be used to predict the sound field in the room. Since the validity of this approach has previously only been demonstrated by numerical simulations (23), in the present work, an experimental investigation is performed.

## 2. THEORY OF ROOM ACOUSTICS EQUIVALENT SOURCES MODEL

### 2.1 Boundary Conditions in Room Acoustics

Equivalent Sources Models were originally developed in the area of acoustical holography (24-25), where the free-space sound field is assumed to be generated by a number of equivalent sources with undetermined strength (sometimes source locations as well (26)), and then the source strengths are estimated by matching the measured sound pressure at different locations. In contrast, the room acoustics equivalent source model first uses the equivalent sources to represent the room component of the total sound field in the room, instead of the free-space sound field, and then uses the impedance boundary conditions on the source and the room surfaces to estimate the source strengths of the equivalent sources, instead of the pressure boundary condition. The boundary conditions used in the room acoustics equivalent source models are as follows (the details of the derivation can be found in references (22- 23)):

$$\begin{cases} \beta_1(x)p_r(x) - u_{nr}(x) = 0 & x \in \Gamma_1 \\ \beta_2(x)p_r(x) - u_{nr}(x) = u_{nf}(x) - \beta_2(x)p_f(x) & x \in \Gamma_2 \end{cases} \quad (1)$$

where  $\Gamma_1$  and  $\Gamma_2$  denote the source surface and the room surface, respectively;  $p_f$  and  $u_{nf}$  are the free-space sound pressure and normal particle velocity;  $p_r$  and  $u_{nr}$  denote the sound pressure and the normal particle velocity of the room component sound field (defined as the total sound field minus the free-space sound field);  $\beta_1$  and  $\beta_2$  are the normal admittance distribution on the source and the room surfaces (and the surfaces are assumed to be locally reacting).

In a typical room acoustics simulation, the free-space information,  $p_f$  and  $u_{nf}$ , are given as well as the surface admittances,  $\beta_1$  and  $\beta_2$ . Thus the simulation of the sound field in the room is accomplished if the room component sound field can be predicted, which is performed by using an equivalent source formulation of the room component.

### 2.2 Model Formulation

To formulate an Equivalent Source Model for room acoustics, a set of equivalent sources with the property of completeness are first selected to describe the room component sound field, i.e., it is required that any possible solution to the Helmholtz equation in the room region can be expressed as a linear combination of the sound field of the equivalent sources in the set with appropriate source strengths for each source. There are various types of equivalent sources with such a completeness property that can be used for the model formulation, such as a distribution of monopoles or dipoles, the series of plane waves, cylindrical waves, spherical waves or multipoles, etc. The difference between the room acoustics Equivalent Sources Models from that used for free-space acoustical holography is that sources representing both out-going and incoming waves need to be included, whereas only out-going sources are required in free-space applications. In general, with a chosen type of equivalent sources, the room component sound field can be expressed as:

$$\begin{cases} p_r(x) = \sum_{i=1}^N g_i(x, y_i) Q_i \\ \vec{u}_r(x) = -\frac{1}{j\omega\rho_0} \sum_{i=1}^N \vec{\nabla} g_i(x, y_i) Q_i \end{cases} \quad (2)$$

where  $p_r$  and  $u_r$  again represent the sound pressure and particle velocity of the room component

sound field,  $g_i(x, y_i)$  is the sound field expression of the  $i$ th equivalent source with unit source strength;  $x$  is the receiver location;  $y_i$  is the location of the  $i$ th source and  $Q_i$  denotes the strength of the  $i$ th source. Here, the time dependence is  $e^{j\omega t}$ ,  $\rho_0$  is the air density and the del represents the gradient operator with respect to  $x$ . It is noted that only a finite number of equivalent sources are included in the model formulation and the higher order sources are discarded.

The goal for this model formulation is to estimate the source strengths,  $Q_i$ , since the sound field expressions,  $g_i(x, y_i)$ , are known as long as the type of equivalent sources are chosen, and then Eq. (2) can be used, along with the calculated source strengths, to predict the sound field at any location in the room. In order to estimate the source strength, a number of sampling points are first chosen on both the source and the room surfaces, and then Eq. (2) is substituted into to Eq. (1) and evaluated at the sampling points, which gives the following matrix formulation:

$$\begin{bmatrix} B_1 A_p^{(1)} - A_{u_n}^{(1)} \\ B_2 A_p^{(2)} - A_{u_n}^{(2)} \end{bmatrix} \vec{Q} = \begin{bmatrix} 0 \\ \vec{u}_{nf} - B_2 \vec{p}_f \end{bmatrix}, \quad (3)$$

with

$$B_1 = \text{diag}(\beta_1(x_1), \beta_1(x_2), \dots, \beta_1(x_{M_1})), \quad B_2 = \text{diag}(\beta_2(x_{M_1+1}), \beta_2(x_{M_1+2}), \dots, \beta_2(x_M)),$$

$$(A_p^{(1)})_{ij} = g_j(x_i, y_j), \quad (A_{u_n}^{(1)})_{ij} = -\frac{1}{j\omega\rho_0} \partial_n g_j(x_i, y_j),$$

$$(A_p^{(2)})_{ij} = g_j(x_{M_1+i}, y_j), \quad (A_{u_n}^{(2)})_{ij} = -\frac{1}{j\omega\rho_0} \partial_n g_j(x_{M_1+i}, y_j),$$

$$\vec{u}_{nf} = [u_{nf}(x_{M_1+1}), u_{nf}(x_{M_1+2}), \dots, u_{nf}(x_M)]^T, \quad \vec{p}_f = [p_f(x_{M_1+1}), p_f(x_{M_1+2}), \dots, p_f(x_M)]^T,$$

where  $x_1, \dots, x_{M_1}$  are the sampling points on the source surface;  $x_{M_1+1}, \dots, x_M$  are the sampling points on the room surface,  $\vec{Q}$  is a vector containing  $Q_1, \dots, Q_N$ , and  $\partial_n$  represents the directional derivative in the surface normal direction. The number of sampling points is usually chosen to be greater than the number of equivalent sources to form an over-determined system and to accurately represent the spatial distribution of the impedance on the surfaces.

The source strength  $\vec{Q}$  can be estimated by finding a least-square solution to the above linear system, Eq. (3), which can then be used to predict the sound field in the room. This formulation is valid for different choices of equivalent source types, as long as the sound field expressions,  $g_i(x, y_i)$ , for the chosen sources are used. In the present work, the series of spherical waves are used as the equivalent sources, i.e., the Bessel function of the first and the second kind multiplied by the spherical harmonics.

### 3. Experimental Validation

#### 3.1 Experiment Setup

In the experimental validation of the room acoustics Equivalent Source Model, a measurement of the sound field generated by a loudspeaker was conducted in a small room with a non-uniform impedance distribution on its surfaces. The predicted sound pressure was then compared with the measured sound pressure at the receiver locations to indicate the performance of the model. The loudspeaker used in the experiment was Infinity Primus P163 with the dimension  $0.265 \text{ m} \times 0.207 \text{ m} \times 0.37 \text{ m}$ ; it was placed in a rectangular-shaped room ( $1.867 \text{ m} \times 1.771 \text{ m} \times 1.950 \text{ m}$ ) with all the surfaces of the loudspeaker parallel to the corresponding surfaces of the room. The setup of the experiment and the geometrical relation between the loudspeaker and the room are illustrated in Figures 1 and 2, where the distance between the back face of the loudspeaker to that of the room is 0.858 m; the distance between the right face of the loudspeaker and that of the room is 0.775m; the distance the two bottom faces is 1.00 m. The surfaces of the room were covered by plywood panels which were then partially covered by sound absorbing materials (Johns Manville, Microlite AA Premium NR Blankets) of 1 inch thickness. The uncovered regions are highlighted in the left figure in Figure 2. The sound field was measured by using a 18-channel planar array (Brüel & Kjær, sliced wheel array WA-1558-W; microphones: Brüel & Kjær,

Type 4959), at four sides of the loudspeaker (measurement planes were parallel to the front, left, back and right faces of the loudspeaker). As shown in Figure 3, there were two measurements on each side: one at a distance of 0.25 m away from the corresponding loudspeaker face and the other at a distance of 0.5 m. The sound field was measured separately on each measurement plane with a white noise input signal to the loudspeaker, and the individual measurements were then synchronized together to form a simultaneous measurement by using the transfer function method (27) with the input signal to the loudspeaker as the reference signal.



Figure 1 – Setup of the experiment.

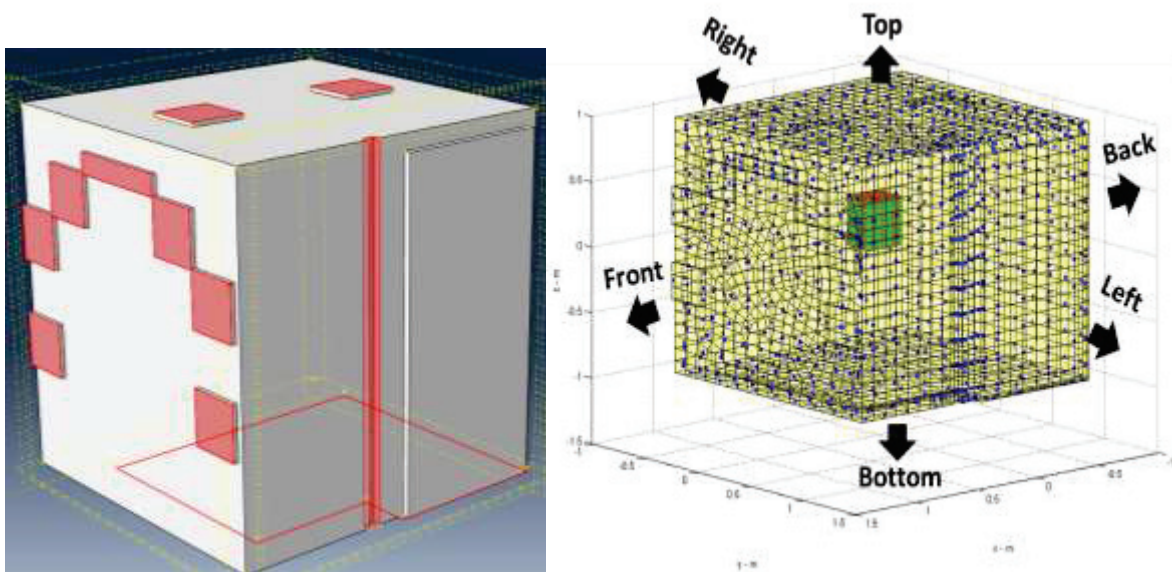


Figure 2 – Left: room geometry (highlighted regions are not covered by sound absorbing materials); Right: geometry relation of the loudspeaker (green) and the room (yellow) and the sampling points on the source surface (red) and the room surface (blue) that were used in the Equivalent Sources Model.

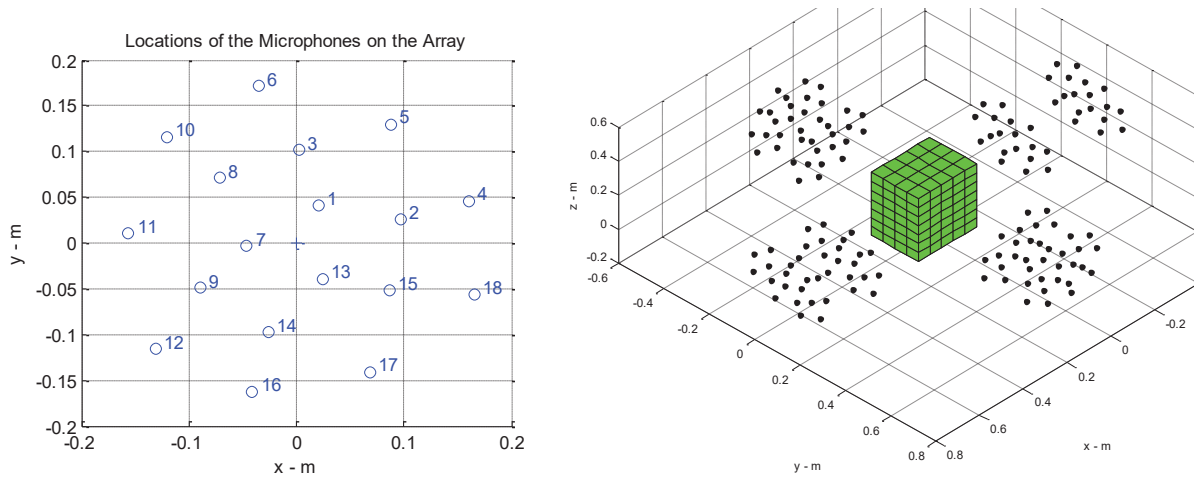


Figure 3 – Left: the receiver locations on the array; Right: the receiver locations (black dots) in the whole measurement (the green box represents the loudspeaker).

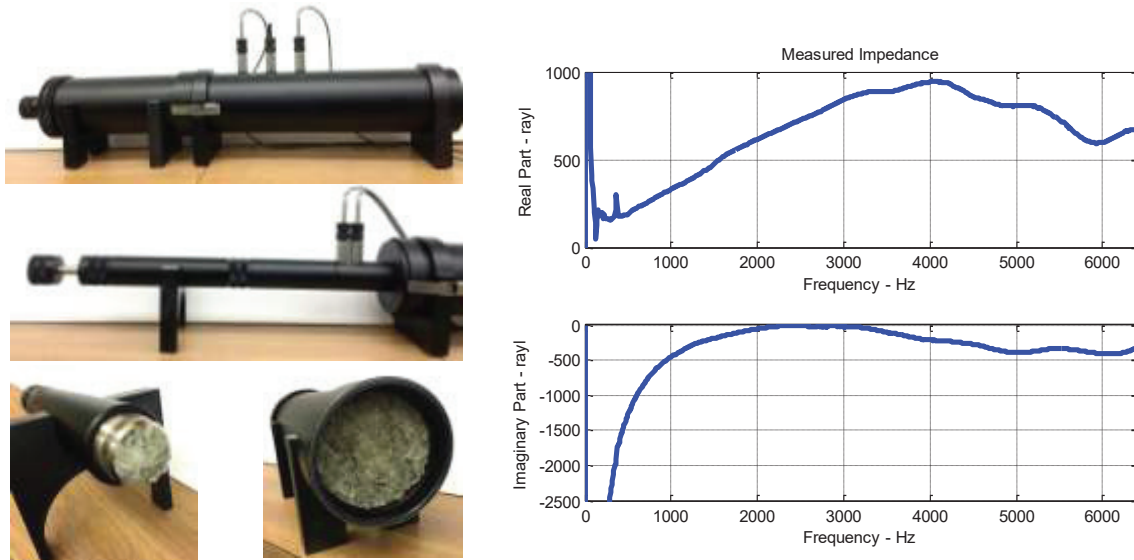


Figure 4 – The setup and results of the impedance measurement.

The normal specific acoustic impedance of the sound absorbing material on a hard surface was measured by using the two-microphone method (28) in an standing wave tube (Brüel & Kjær, Type 4206). This measured impedance was used as the impedance boundary condition, under the assumption of local reaction, for the covered surfaces of the room. The setup and the result of the impedance measurement are shown in Figure 4. The uncovered plywood surfaces were considered to be acoustically hard surfaces. For the boundary condition on the loudspeaker surface, it was assumed that the normal velocity distribution on the source surface was the same as in the free-space environment: i.e., it was assumed that the sound reflected from the room surface caused negligible velocity change on the loudspeaker surface. To apply the latter velocity boundary condition, it is only necessary to set  $\beta_1 = 0$  in Eq. (1). The velocity distribution on the source surface was calculated by a free-space Multipole Equivalent Sources Model (26) obtained from another sound pressure measurement of the same loudspeaker in an anechoic environment. Thus the simulation in the present work involves using a free-space Equivalent Sources Model as an input to an the room acoustics Equivalent Sources Model.

### 3.2 Measurement Results and Discussion

After determining the boundary conditions on the different surfaces, the sound field in the room can be simulated by using the room acoustics Equivalent Sources Model described in Section 2. The equivalent sources used in the present work are the spherical waves up to order three. To calculate the source strengths, 487 sampling points on the room surface and 166 sampling points on the source

surface were used (illustrated in Figure 2). The model-predicted sound pressure is compared with the measured sound pressure at all the receiver locations, and the comparison results are shown at 520 Hz, 1024 Hz and 2000 Hz in Figures 5 to 10, where the receiver indices are ordered such that receiver indices 1 to 72 correspond to the measurements with a smaller distance (0.25 m) to the source, and 73 to 144 with a distance of 0.5 m; while at each measurement distance the 72 indices are ordered as front face measurement, left face, back face and then right face.

From the comparison results, it is seen that the Equivalent Sources Model (ESM) prediction does not agree well with the experiment result at 520 Hz. Although better agreement is seen at higher frequencies (1024 Hz and 2000 Hz), that does not necessarily indicate good model performance since the total sound field is close to the free-space sound field at these frequencies, which suggests that good model prediction occurs simply because the room surface is very absorptive at higher frequencies and the room component sound field is close to zero. Overall, the ESM prediction tends to be close to the free-space sound field.

To further analyze the reason for this result, a simulation using the Boundary Element Model (BEM) was carried out at 520 Hz, in which there were 3438 nodes in the mesh (more than 6 nodes per wave length). From Figure 11, it is first noticed that the BEM prediction agrees reasonably well with the experiment. Also from the BEM calculation, the sound pressure and the normal particle velocity distribution of the room component sound field (i.e., the component that is represented by ESM) can be extracted for both the room surface and the source surface. With this information extracted from BEM, the source strengths of the ESM (with the same model structure as the ESM described in the previous paragraph) can be estimated based on three different types of boundary condition: the room component pressure boundary condition, the normal velocity boundary condition and the impedance boundary condition (Eq. (3)). By comparing the performance of the ESM's with these three boundary conditions, it is observed that the prediction using the pressure boundary condition shows a fairly good agreement with the BEM and the experiment results, while the other two boundary conditions result in predictions that are close to each other and are, as seen from Figure 5, both close to the free-space sound field. These observations imply that it is valid to use a small number of higher order equivalent sources to represent the room component sound field, and that the use of the velocity boundary condition to calibrate the ESM is more likely to produce errors in sound pressure predictions. For the prediction from the impedance boundary condition, its formulation, as seen from Eq. (3), is a linear combination of the pressure and the velocity boundary condition, so the least squares estimate is essentially a weighted least square estimate that combines the results from the other two boundary conditions. The admittance serves as the weighting factor of the result from the pressure boundary condition, while the weighting factor for the velocity boundary condition is unity. Since, from Figure 4, the impedance is on the order of  $10^3$ , the weighting factors for the pressure boundary condition (on the order of  $10^{-3}$  for the material covered surfaces and zero for the hard surfaces) are very small compared with unity. This causes the prediction from Eq. (3) to be closer to the prediction from the velocity boundary condition which produces large errors. This means that for cases where the admittance is small, the direct use of the least square estimate from Eq. (3) may produce large errors in the room acoustics predictions.

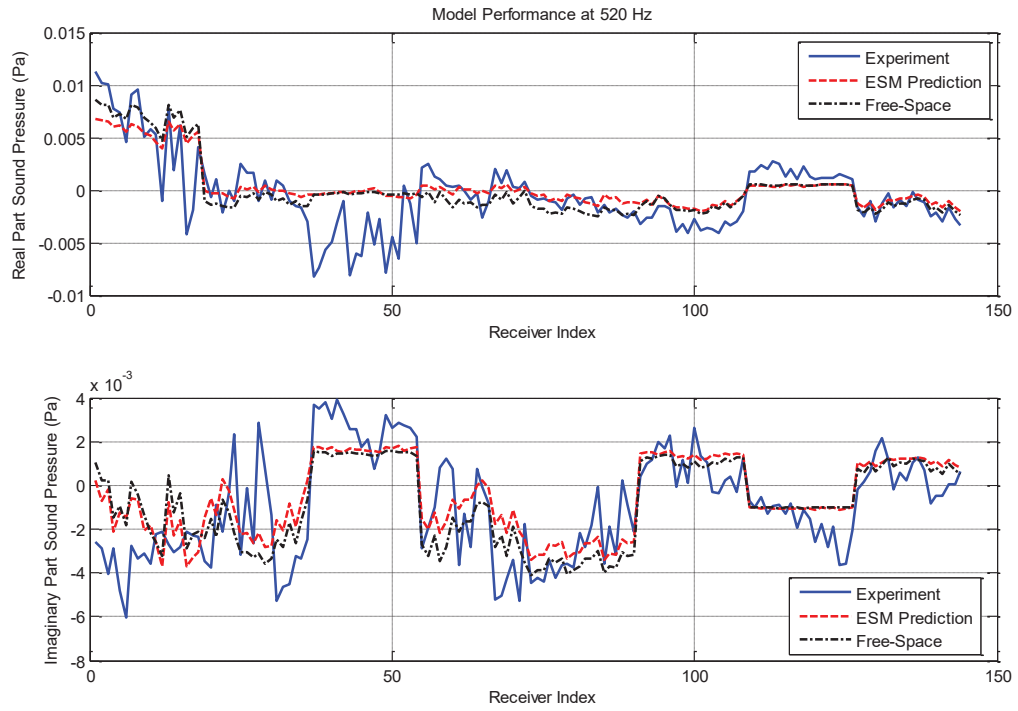


Figure 5 – Comparison of measurement and model prediction at 520 Hz (plot with receiver indices).

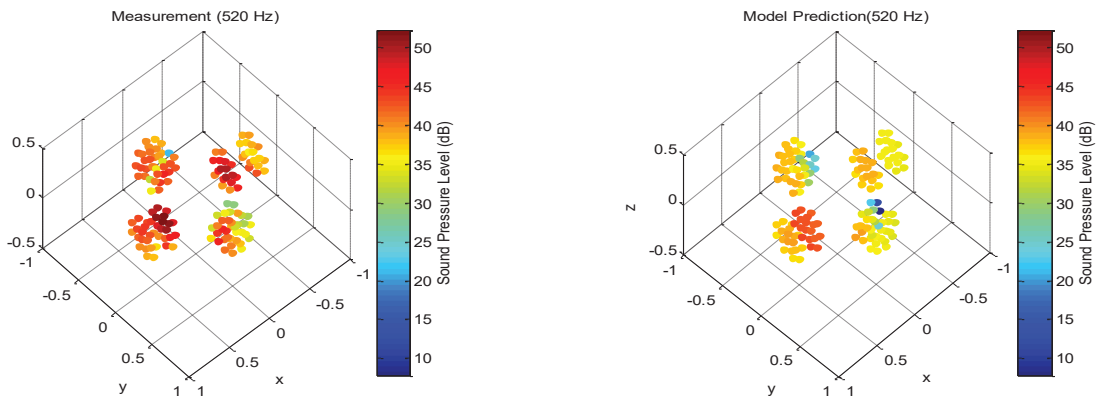


Figure 6 – Comparison of measurement and model prediction at 520 Hz (spatial distribution).

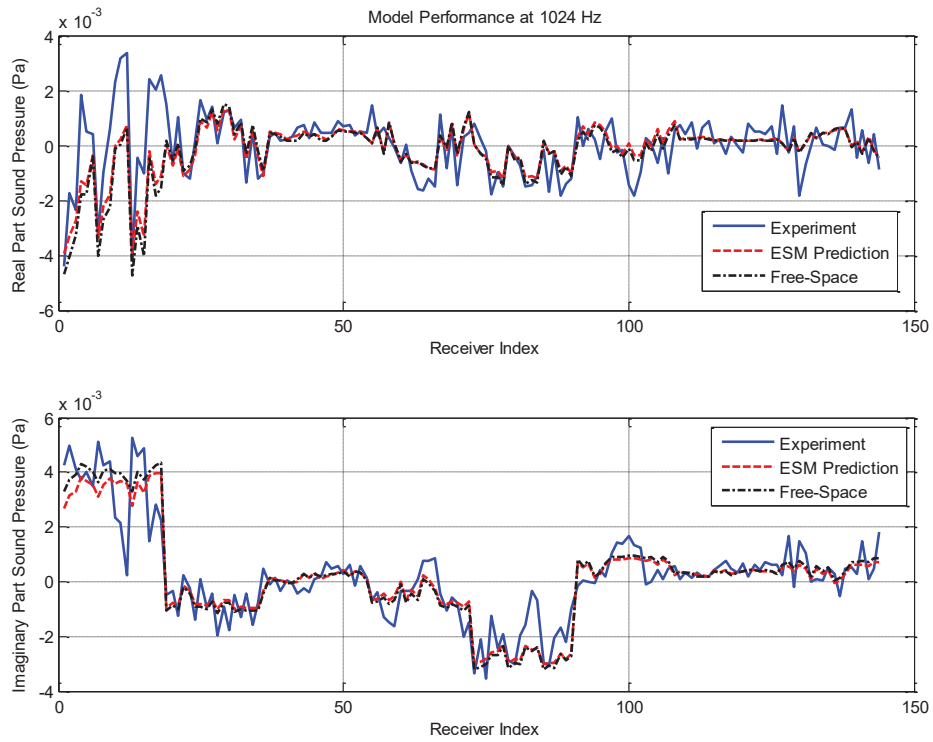


Figure 7 – Comparison of measurement and model prediction at 1024 Hz (plot with receiver indices).

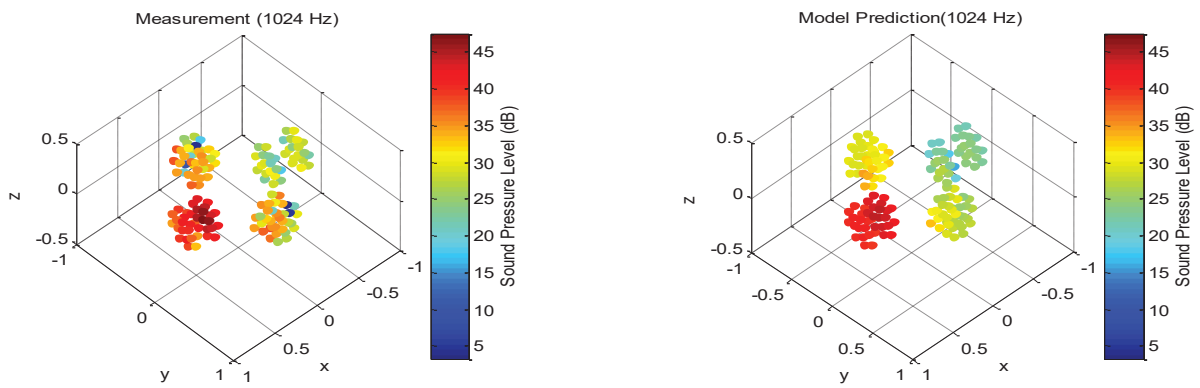


Figure 8 – Comparison of measurement and model prediction at 1024 Hz (spatial distribution).



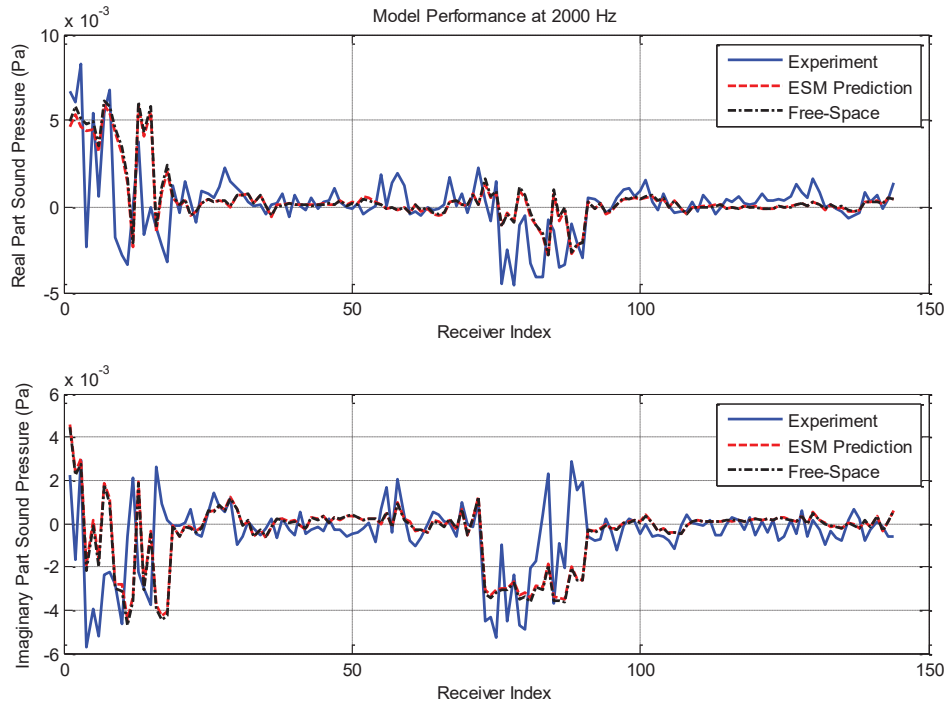


Figure 9 – Comparison of measurement and model prediction at 2000 Hz (plot with receiver indices).

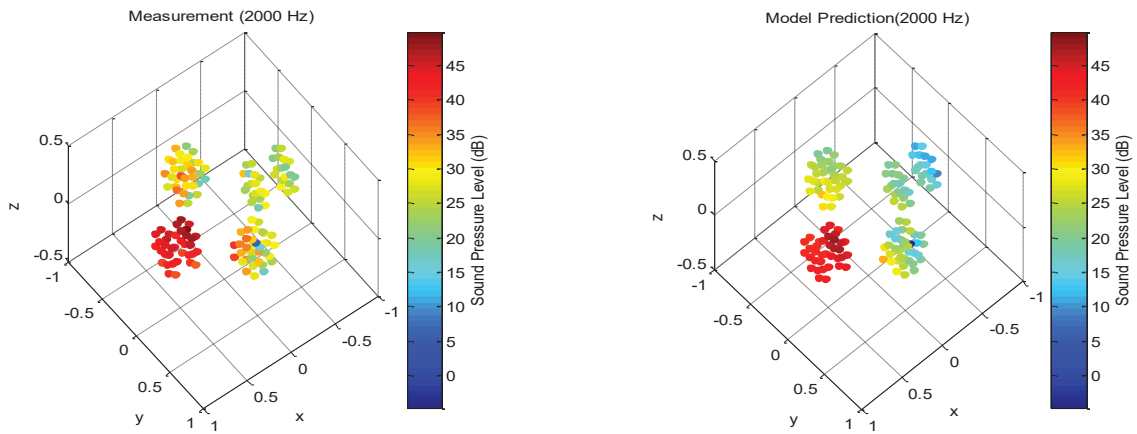


Figure 10 – Comparison of measurement and model prediction at 2000 Hz (spatial distribution).

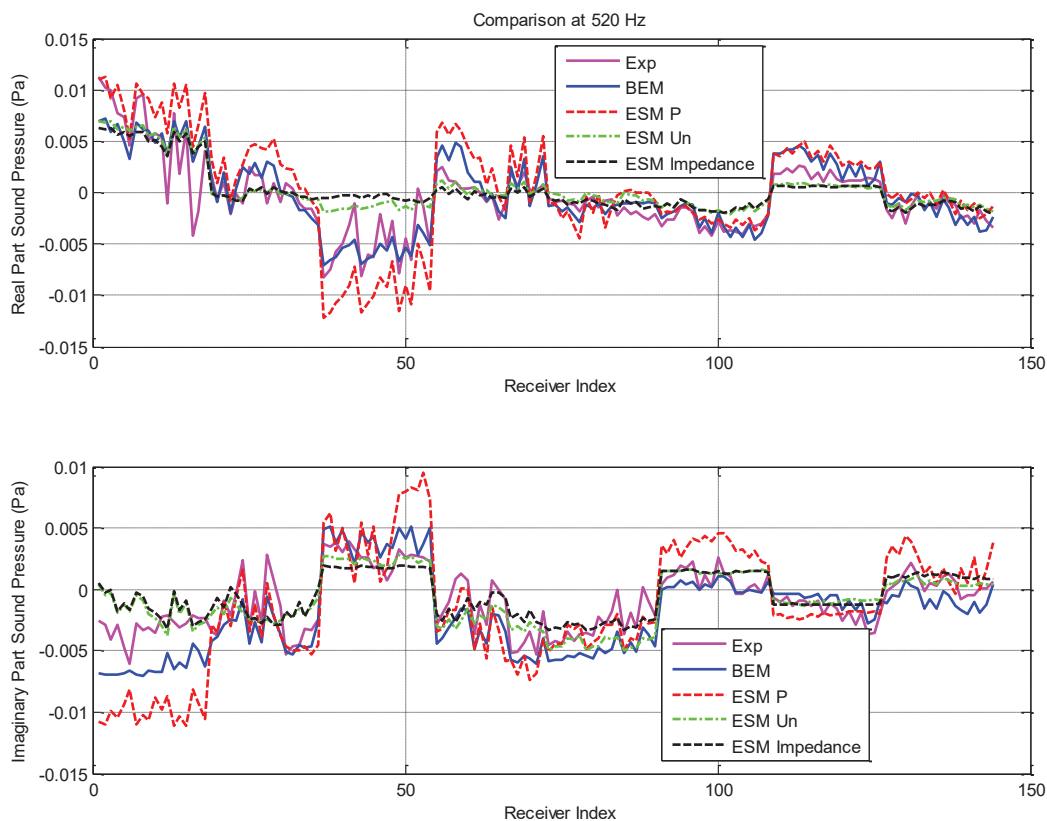


Figure 11 – Comparison of model performance of BEM and ESM based on different types of boundary conditions (pressure, velocity and impedance boundary conditions) at 520 Hz.

#### 4. SUMMARY

The recently developed room acoustics Equivalent Sources Model was experimentally investigated in the present work. From the results, it was shown that the Equivalent Source Model prediction can achieve reasonable accuracy if the sound pressure boundary condition of the room component sound field is used to calibrate the model, but if the normal velocity boundary condition is used, the sound pressure prediction may contain large errors. In realistic room acoustics simulation practice, the available boundary condition is the impedance boundary condition, and if a direct least-squares estimate is used for calculating the strength of the equivalent sources, the prediction from the impedance boundary condition results in a weighted combination of the results from the pressure and the velocity boundary conditions where the value of the admittance is the relative weighting factor for the pressure boundary condition result. For the experimental condition in the present work, the admittance is small compared with one, which leads to a model prediction that is close to the result using the velocity boundary condition.

#### REFERENCES

1. Veronesi WA, Maynard JD. Digital holographic reconstruction of sources with arbitrarily shaped surfaces. *J Acoust Soc Am*. 1989;85(2):588-598.
2. Bai MR. Application of BEM (boundary element method)-based acoustic holography to radiation analysis of sound sources with arbitrarily shaped geometries. *J Acoust Soc Am*. 1992;92(1):533-549.
3. Kim BK, Ih JG. On the reconstruction of the vibro-acoustic field over the surface enclosing an interior space using the boundary element method. *J Acoust Soc Am*. 1996;100(5):3003-3016.
4. Granier E, Kleiner M, Dalenback BI, Svensson P. Experimental Auralization of car audio installations. *J Audio Eng Soc*. 1996;44(10):835-849.
5. Van Hal B, Desmet W, Vandepitte D, Sas P. A coupled finite element-wave-based approach for the steady-state dynamic analysis of acoustics systems. *J Comp Acous*. 2003;11(2):285-303.
6. Van Genechten B, Pluymers B, Vandepitte D, Desmet W. Hybrid wave based-modally reduced finite

- element method for the efficient analysis of low-and mid-frequency car cavity acoustics. *SAE Int J Passeng Cars - Mech Syst.* 2009;2(1):1494-1504.
7. Mechel FP. Improved mirror source method in room acoustics. *J Sound Vib.* 2002;256(5):873-940.
  8. Dalenbäck BI, McGrath D. Narrowing the gap between virtual reality and auralization. *Proc 15th ICA;* 26-30 June 1995; Trondheim Norway 1995. vol. 2. p. 429-432.
  9. Rindel JH, Christensen CI. Room acoustic simulation and auralization – how close can we get to the real room. *Proc 8th Western Pacific Acoustics Conference;* 7-9 April 2003; Melbourne, Australia 2003. CD-ROOM 8.
  10. Stephenson UM. Quantized beam tracing - a new algorithm for room acoustics and noise immission prognosis. *Acta Acustica united with Acustica.* 1996;82(3):517-525.
  11. Allen JB, Berkley DA. Image method for efficiently simulating small-room acoustics. *J Acoust Soc Am.* 1979;65(4):943-950.
  12. Borish J. Extension of the image model to arbitrary polyhedra. *J Acoust Soc Am.* 1984;75(6):1827-1836.
  13. Gibbs BM, Jones DK. A simple image model for calculating the distribution of sound pressure levels within an enclosure. *Acustica.* 1972;26(1):24-32.
  14. Krokstad A, Storm S, Sorsdal S. Calculating the acoustical room response by the use of a ray tracing technique. *J Sound Vib.* 1968;8(1):118-125.
  15. Schroeder MR. Digital simulation of sound transmission in reverberant spaces. *J Acoust Soc Am.* 1970;46(2):424-431.
  16. Haviland JK, Thanedar BD. Monte Carlo applications to acoustical field simulations. *J Acoust Soc Am.* 1973;54(6):1442-1448.
  17. Dadoun N, Kirkpatrick D, Walsh J. The geometry of beam tracing. *Proc 1st Annual Symposium on Computational Geometry SSG 85;* 05-07 June 1985; Baltimore, USA 1985. ACM Press, New York, 1985. p. 55-61.
  18. Van Maercke D, Martin J. The prediction of echograms and impulse responses within the Epidaur software. *Appl Acoust.* 1993;38(2-4):93-114.
  19. Dalenbäck BI. Room acoustic prediction based on a unified treatment of diffuse and specular reflection. *J Acoust Soc Am.* 1996;100(2):899-909.
  20. Rindel H. Modelling the angle-dependent pressure reflection factor. *Appl Acoust.* 1993;38(2):223-234.
  21. Vorlander M. Simulation of transient and steady-state sound propagation in rooms using a new combined ray-tracing/image-source algorithm. *J Acoust Soc Am.* 1989;86(1):172-178.
  22. Liu Y, Bolton JS. The use of equivalent source models for reduced order simulation in room acoustics. *Proc Meetings of Acoustics 2013;* 02-07 June 2013; Acoustical Society of America. 2013;19(1): p. 015130.
  23. Liu Y, Bolton JS. Simulation of sound fields radiated by finite-size sources in room environments by using equivalent source models: three-dimensional validation. *Proc INTER-NOISE and NOISE-CON 2015;* 9-12 August 2015; San Francisco, USA 2015. 250(3): p. 4246-4259.
  24. Koopman GH, Song L, Fahnlne JB. A method for computing acoustic fields based on the principle of wave superposition. *J Acoust Soc Am.* 1989; 86(6):2433-2438.
  25. Wang Z, Wu SF. Helmholtz Equation-Least Squares method for reconstructing the acoustic pressure field. *J Acoust Soc Am.* 1997; 102(4):2020-2032.
  26. Liu Y, Bolton JS. The use of non-collocated higher order sources in the equivalent source method. *Proc INTER-NOISE and NOISE-CON 2012;* 19-22 August 2012; New York, USA 2012. 2012(4): p. 7326-7337.
  27. Kim YJ, Bolton JS, Kwon HS. Partial sound field decomposition in multireference near-field acoustical holography by using optimally located virtual references. *J Acoust Soc Am.* 2004; 115(4):1641-1652.
  28. Standard ISO. 10534-2: Determination of sound absorption coefficient and impedance in impedance tubes.